SCIENCE CHINA
Information Sciences

• **Supplementary File** •

Plug-and-Play algorithm for under-sampling Fourier single-pixel imaging

Ye Tian[1,3], Ying Fu[2*] & Jun Zhang[1,3]

[1]*School of Information and Electronics, Beijing Institute of Technology, Beijing* 100081*, China;*
[2]*School of Computer Science and Technology, Beijing Institute of Technology, Beijing* 100081*, China;*
[3]*Advanced Research Institute of Multidisciplinary Science, Beijing Institute of Technology, Beijing* 100081*, China*

Appendix A Plug-and-Play based FSI algorithm

The PnP–FSI algorithm is exhibited in Algorithm A1.

Algorithm A1 PnP–FSI

Input: I_m.
Output: Reconstructed Imagine O^{k+1}.
1: Initial O^0, Z^0, λ.
2: **for** $k = 1$ to K **do**
3: $O^{k+1} = Z^k + \mathscr{F}^{-1}(I_m - \mathscr{F}(Z^k))$;
4: $Z^{k+1} = \mathcal{D}_\sigma(O^{k+1})$, where $\sigma = \sqrt{\lambda}$;
5: **end for**

Appendix B Experimental results

Appendix B.1 Simulation settings

A series of numerical simulations and experiments are conducted to validate the performance of our proposed method. We compare the imaging quality of three under-sampling FSI reconstruction methods, including low-resolution sampling method (LR), variable density random under-sampling with CS method (VCS) and our proposed PnP–FSI method. The LR method [1] refers to only sampling low-frequency components in the circular sampling order and reconstructing image by inverse Fourier transform. The VCS method is the sparse Fourier single-pixel imaging based on CS algorithm [2]. For our proposed PnP–FSI method, we choose the FFDNet [3] as the denoiser. Both the VCS method and our proposed PnP–FSI method use variable density random sampling scheme. For variable density random sampling scheme, the parameters are $D = 0.3$ and $p = 4$ as the sampling ratio is higher than 0.2. While for sampling ratio lower than 0.2, the parameters are set as $D = 0.2$ and $p = 8$. There are three main metrics for evaluating the quality of the reconstructed image, *i.e.*, Peak Signal-to-Noise Ratio (PSNR), Structural Similarity Index (SSIM) and Root Mean Square Error (RMSE). Generally, larger PSNR and SSIM, smaller RMSE suggest a better FSI reconstruction.

Appendix B.2 Numerical simulations

In simulation, we use the Set12 dataset [4] as the target scenes. The sampling ratios are set from 8% to 50% and the image sizes of 64×64, 96×96, 128×128, 256×256 are considered. The simulated results are shown in Table B1. It can be observed that the proposed PnP–FSI algorithm has higher FSI reconstruction quality compared with LR method and VCS method in the case of under-sampling. To visualize the image reconstruction quality, we show images of the "cameraman" reconstructed by different algorithms at various image sizes and sampling ratios in Fig. B1. In order to display the image details more clearly, we intercept the same part of all reconstructed images. It can be seen that the proposed algorithm can achieve more image details and clear edges in the under-sampling situation. In contrast, the LR method loses a large number of image details and has ringing effect in the reconstructed images. The VSC method recovers a part of image details but it brings watercolor-like artifacts in the reconstructed images. In addition, as the image size increases, our algorithm still keeps a higher performance, and thus it is suitable for lager-size under-sampling SPI reconstruction.

Next, we investigate the noise robustness of the proposed algorithm by adding white Gaussian noise to FSI measurements in simulation. The white Gaussian noise can be expressed as:

$$P(N) = \frac{1}{\sqrt{2\pi}\sigma} exp(-\frac{N^2}{2\sigma^2}), \tag{B1}$$

* Corresponding author (email: fuying@bit.edu.cn)

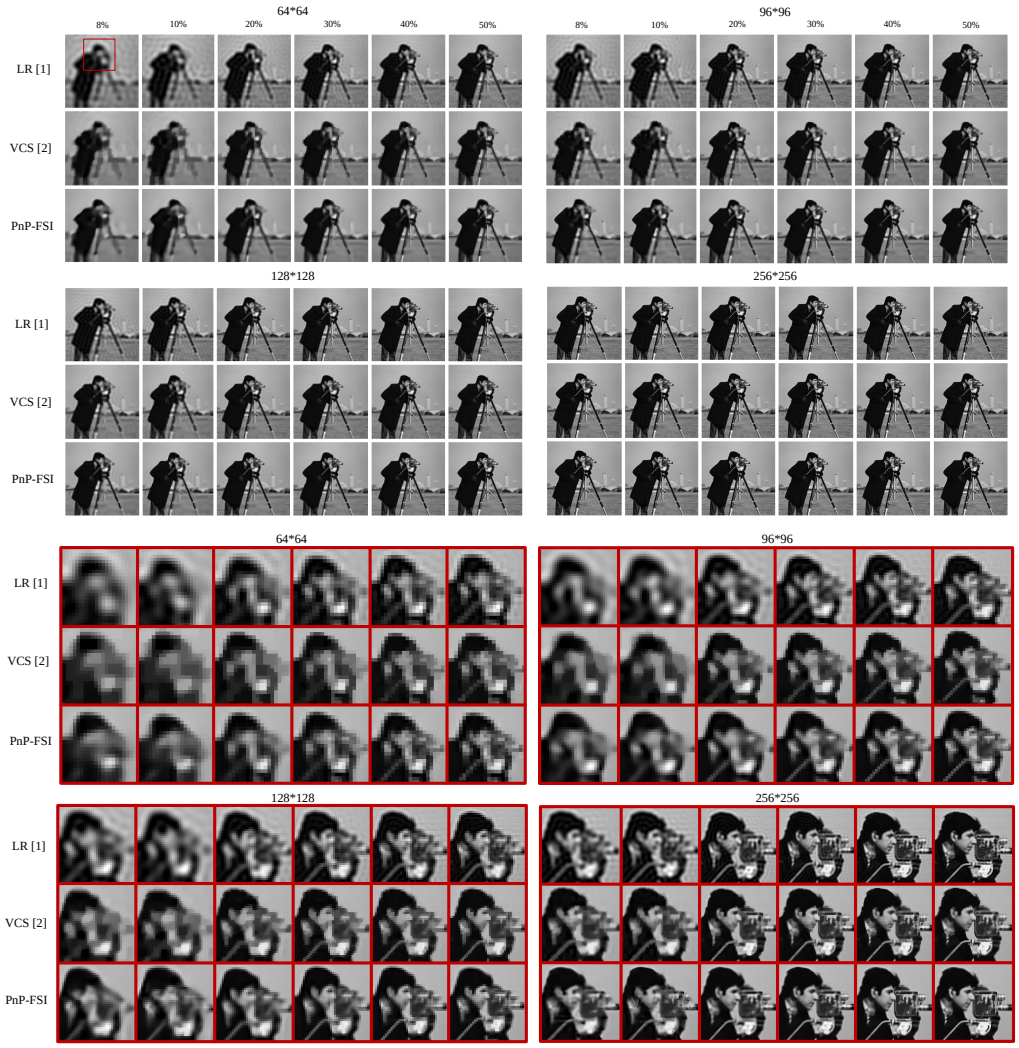

Figure B1 "Cameraman" images reconstructed by different under-sampling FSI reconstruction methods.

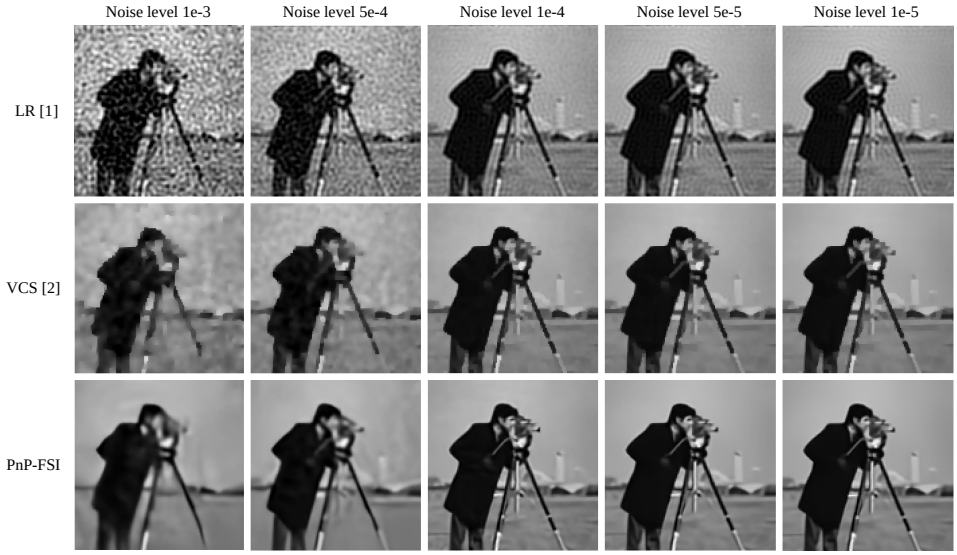

Figure B2 "Cameraman" images (128 × 128) reconstructed by different under-sampling FSI reconstruction methods with different noise levels.

Table B1 Average PSNR, SSIM and RMSE of Set12 images reconstruction with different sampling ratios.

Image size	Algorithm		8%	10%	20%	30%	40%	50%
64 × 64	LR [1]	PSNR	21.80	22.55	25.25	27.14	29.23	31.17
		SSIM	0.6418	0.6908	0.8242	0.8781	0.9190	0.9431
		RMSE	0.0824	0.0757	0.0554	0.0445	0.0349	0.0279
	VCS [2]	PSNR	21.94	22.13	25.28	26.61	28.43	30.35
		SSIM	0.6613	0.6691	0.8315	0.8615	0.8963	0.9255
		RMSE	0.0815	0.0798	0.0560	0.0484	0.0396	0.0319
	PnP–FSI	PSNR	**22.51**	**22.93**	**26.33**	**28.05**	**29.94**	**31.70**
		SSIM	**0.7017**	**0.7201**	**0.8631**	**0.8973**	**0.9245**	**0.9432**
		RMSE	**0.0764**	**0.0731**	**0.0491**	**0.0403**	**0.0325**	**0.0266**
96 × 96	LR [1]	PSNR	22.92	23.63	26.33	28.57	30.45	32.36
		SSIM	0.6845	0.7260	0.8376	0.8941	0.9271	0.9484
		RMSE	0.0724	0.0667	0.0487	0.0376	0.0303	0.0243
	VCS [2]	PSNR	23.06	23.24	26.70	28.35	30.08	32.21
		SSIM	0.7075	0.7125	0.8629	0.8891	0.9135	0.9381
		RMSE	0.0717	0.0702	0.0471	0.0392	0.0321	0.0253
	PnP–FSI	PSNR	**23.84**	**24.71**	**27.79**	**29.62**	**31.24**	**34.55**
		SSIM	**0.7472**	**0.7933**	**0.8863**	**0.9108**	**0.9291**	**0.9593**
		RMSE	**0.0657**	**0.0594**	**0.0414**	**0.0336**	**0.0279**	**0.0196**
128 × 128	LR [1]	PSNR	23.80	24.64	27.40	29.46	31.45	33.44
		SSIM	0.7140	0.7546	0.8561	0.9034	0.9329	0.9530
		RMSE	0.0652	0.0592	0.0431	0.0340	0.0270	0.0215
	VCS [2]	PSNR	24.07	24.30	28.12	29.76	31.73	33.84
		SSIM	0.7456	0.7492	0.8826	0.9039	0.9269	0.9474
		RMSE	0.0635	0.0619	0.0400	0.0332	0.0266	0.0210
	PnP–FSI	PSNR	**25.04**	**25.59**	**29.51**	**30.81**	**32.46**	**36.25**
		SSIM	**0.7869**	**0.8013**	**0.9025**	**0.9179**	**0.9342**	**0.9655**
		RMSE	**0.0571**	**0.0538**	**0.0341**	**0.0294**	**0.0243**	**0.0158**
256 × 256	LR [1]	PSNR	25.70	26.41	28.97	31.03	32.83	34.75
		SSIM	0.7565	0.7856	0.8686	0.9088	0.9328	0.9513
		RMSE	0.0526	0.0486	0.0363	0.0288	0.0236	0.0191
	VCS [2]	PSNR	26.28	26.51	30.02	31.94	33.76	35.68
		SSIM	0.7859	0.7910	0.8891	0.9111	0.9298	0.9474
		RMSE	0.0496	0.0483	0.0321	0.0257	0.0208	0.0167
	PnP–FSI	PSNR	**27.29**	**27.74**	**30.86**	**33.69**	**35.39**	**37.56**
		SSIM	**0.8180**	**0.8266**	**0.8949**	**0.9298**	**0.9446**	**0.9584**
		RMSE	**0.0440**	**0.0418**	**0.0290**	**0.0210**	**0.0173**	**0.0133**

Table B2 Average PSNR, SSIM and RMSE of Set12 images (128 × 128) reconstruction with different measurement noise levels.

Algorithm		1e-3	5e-4	1e-4	5e-5	1e-5
LR [1]	PSNR	18.12	22.84	27.07	27.32	27.40
	SSIM	0.3821	0.5862	0.8319	0.8498	0.8559
	RMSE	0.1240	0.0721	0.0446	0.0435	0.0431
VCS [2]	PSNR	21.75	23.82	26.99	27.16	27.20
	SSIM	0.5750	0.7116	0.8496	0.8534	0.8547
	RMSE	0.0820	0.0648	0.0452	0.0444	0.0442
PnP–FSI	PSNR	**22.92**	**25.14**	**29.15**	**29.42**	**29.50**
	SSIM	**0.6828**	**0.7792**	**0.8965**	**0.9014**	**0.9024**
	RMSE	**0.0719**	**0.0559**	**0.0355**	**0.0345**	**0.0341**

where σ is standard deviation. The noise level defined as the ratio between σ and pixel numbers which set as $1e-3$ to $1e-5$. The sampling ratio is fixed to 20% and the image size is 128×128. The simulated results are shown in Table B2. As shown in Table B2, with increase of the noise level, all the test algorithms show the deterioration of performance. Nevertheless, for a given noise level, the proposed PnP–FSI algorithm has higher PSNR and SSIM as well as lower RMSE, which indicates a better image reconstruction quality. Meanwhile, it can be observed that when the noise level is lower than $1e-4$, the indicators of the test algorithms are slight worsen with increase of the noise level. As the noise lever rises further, the LR method degenerates significantly, while our proposed PnP–FSI algorithm still remains a relatively high performance. These results demonstrate that the proposed algorithm

Table B3 Running time in seconds of different algorithms.

Algorithm	64 × 64	96 × 96	128 × 128	256 × 256
LR [1]	0.28	1.20	2.81	44.22
VCS [2]	3.72	16.96	40.05	609.39
PnP–FSI	2.62	5.59	10.11	190.97

is more robust to noise. To visualize the image reconstruction quality, Fig. B2 shows the pictures of "cameraman" reconstructed at different measurement noise levels. It can be seen that our proposed algorithm behaves higher performance than other methods. With the increase of noise level, ringing effect of LR method and the watercolor-like artifacts of VCS method become more serious.

To further validate the performance of our proposed PnP–FSI algorithms, we compare the running time of different SPI algorithms as the size of image increases. All algorithms are tested by MatlabR2019b on a computer with Intel Core i7-9700 3.0 GHz CPU, 16G RAM, and 64 bit Windows 10 operating system. The sampling ratio is fixed to 20%. As shown in Table B3, it can be found that our proposed algorithm has slightly longer running time than the LR method, but operates faster than the VCS method.

Appendix B.3 Experimental results

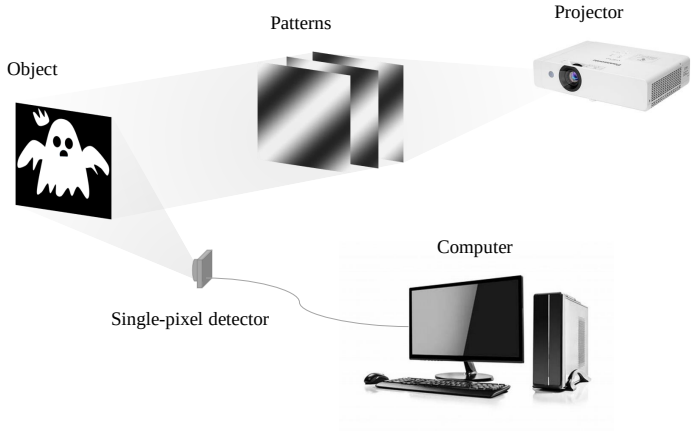

Figure B3 Experimental imaging setup. The projector illuminates the object with a set of Fourier patterns. The single-pixel detector collects the reflected light from the object and feeds the resulting signals to the computer for reconstruction.

We compare different under-sampling FSI algorithms by real experimental data. Two kinds of target scenes are considered, including a 2D image printed on opaque plate and real objects. The experiment setup is shown in Fig. B3. A projector (X416C XGA, Panasonic) is employed to provide spatial light modulation and a photodiode amplifier is used as the single-pixel detector (PDA100A2, Thorlabs) to collect the light reflected from the target image. The sizes of Fourier patterns are 128×128 and sampling ratio is set as 8% to 50%. The experimental results are shown in Fig. B4. Compared with LR method and VCS method, higher quality images are obtained by our proposed PnP–FSI algorithm in FSI, which agree well with the simulation results. In addition, it can be seen that our PnP–FSI algorithm is more robust to noise which makes it suitable for practical SPI application.

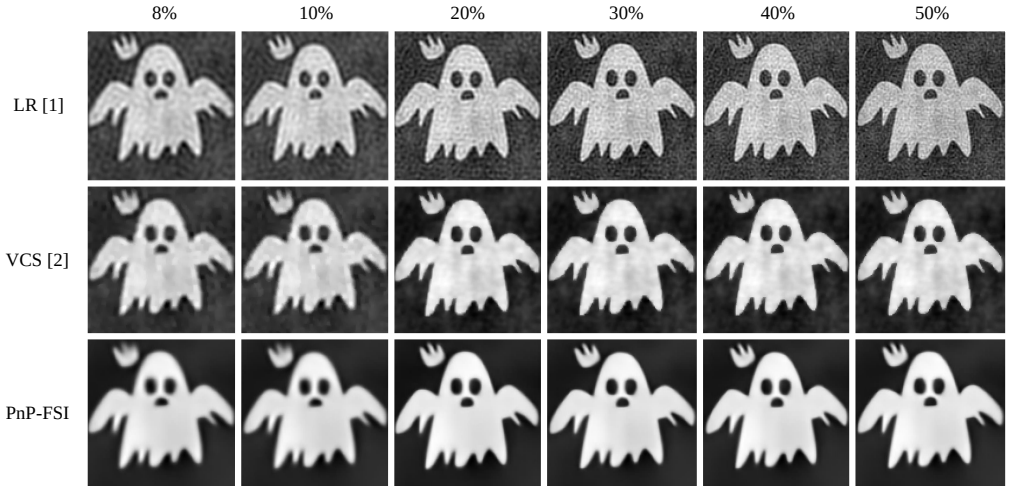

(a)

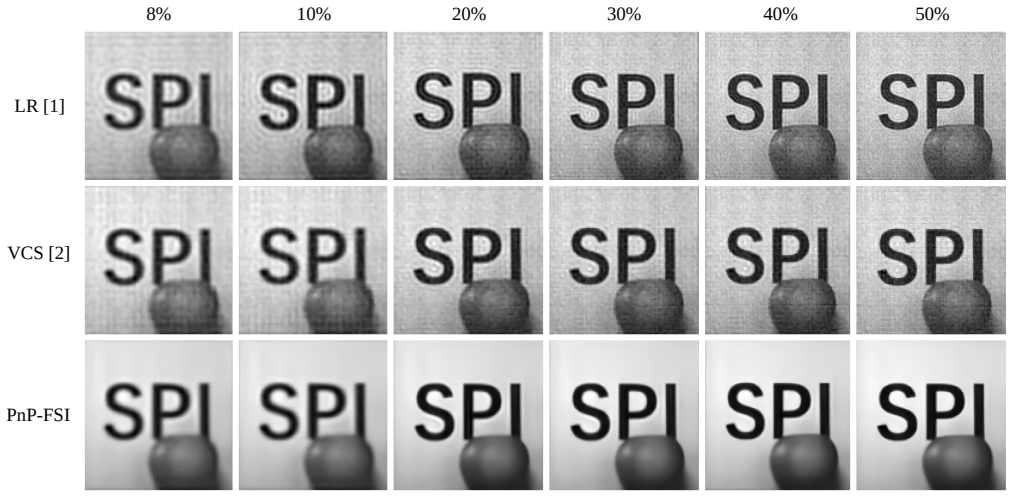

(b)

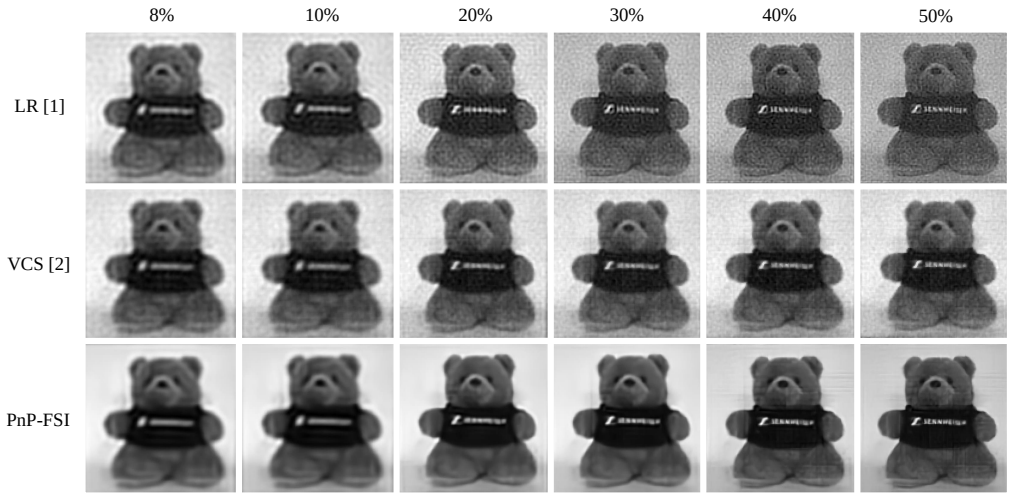

(c)

Figure B4 Experimental results of under-sampling FSI reconstruction obtained by different methods. (a) The reconstructed images of 2D picture. (b) The reconstructed images of an apple with "SPI" letter background. (c) The reconstructed images of a toy bear.

References

1 Zhang Z, Wang X, Zheng G, et al. Hadamard single-pixel imaging versus Fourier single-pixel imaging. Optics Express, 2017, 25: 19619-19639.

2 Meng W W, Shi D F, Huang J, et al. Sparse Fourier single-pixel imaging. Optics express, 2019, 27: 31490-31503.

3 Zhang K, Zuo W, Zhang L. FFDNet: Toward a fast and flexible solution for CNN-based image denoising. IEEE Transactions on Image Processing, 2018, 27: 4608-4622.

4 Zhang K, Li Y, Zuo W, et al. Plug-and-play image restoration with deep denoiser prior. IEEE Transactions on Pattern Analysis and Machine Intelligence, 2021.